Proceedings of ISAP'04, Sendai, JAPAN

PERFORMANCE OF MIMO-SDM IN INDOOR LINE-OF-SIGHT ENVIRONMENTS BASED ON 5.2GHz MEASUREMENTS

Hiroshi NISHIMOTO, Yasutaka OGAWA, Toshihiko NISHIMURA, and Takeo OHGANE
Graduate School of Engineering, Hokkaido University
Kita 13, Nishi 8, Kita-ku Sapporo, 060–8628, Japan
E-mail nishi@niseko.ice.eng.hokudai.ac.jp

1. Introduction

Space division multiplexing (SDM) in a multiple-input multiple-output (MIMO) system (MIMO-SDM), which will provide very high channel capacity in future wireless communications [1], has been studied extensively, and many MIMO measurement campaigns have been conducted [2]–[6]. It is needed to separate and detect the transmitted streams by processing at a receiver end in SDM. It has been reported that the performance of MIMO-SDM is excellent when the channels between transmit and receive antennas are independently and identically distributed (i.i.d.). It is considered that such i.i.d. channels exist in a non-line-of-sight (NLOS) environment with many scatterers. However, actual propagation can have line-of-sight (LOS) environments. A direct wave increases received power, whereas channels may be correlated. In this paper, we present the performance of MIMO-SDM in indoor LOS environments with many scatterers from results of a 5.2GHz measurement campaign.

2. MIMO-SDM Model

Fig. 1 shows a model of MIMO-SDM system. We assume that the system has K transmit (TX) elements and N receive (RX) elements. We also assume that the transmission bandwidth is so narrow that the fading is flat. If independent signal streams are transmitted from each TX antenna, an N-dimensional received signal vector $\boldsymbol{x}(t)$ is given by

$$\boldsymbol{x}(t) = \boldsymbol{H}\boldsymbol{s}(t) + \boldsymbol{n}(t) \; , \tag{1}$$

where $\boldsymbol{s}(t)$ is a K-dimensional transmitted signal vector, and $\boldsymbol{n}(t)$ is an N-dimensional additive white Gaussian noise vector. Also, $\boldsymbol{H}$ is an $N \times K$ MIMO channel matrix, which consists of channels between each TX and RX antenna, and expressed as

$$\boldsymbol{H} = \begin{pmatrix} h_{11} & h_{12} & \cdots & h_{1K} \\ h_{21} & h_{22} & \cdots & h_{2K} \\ \vdots & \vdots & h_{ij} & \vdots \\ h_{N1} & h_{N2} & \cdots & h_{NK} \end{pmatrix} . \tag{2}$$

Here, h_{ij} denotes a channel response from the jth TX antenna to the ith RX one. We formed virtual MIMO systems and obtained matrices $\boldsymbol{H}$ from channel data measured in actual indoor propagation environments. Then, we evaluated the performance.

3. MIMO Measurement Setup

The measurement campaign was conducted at a lounge in the *Hokkaido University Information Electronics Research Building* as shown in Fig. 2. The lounge is a space in the center of the 11th floor in the building. Offices are aligned along the hallways. The wall is made of reinforced

This work was supported in part by Strategic Information and Communications R&D Promotion Programme (SCOPE), Ministry of Public Management, Home Affairs, Posts and Telecommunications, and Grant-in-Aid for Scientific Research (B)(2), 15360198, Japan Society for the Promotion of Science.

ISBN: 4-88552-206-4 C3055©IEICE

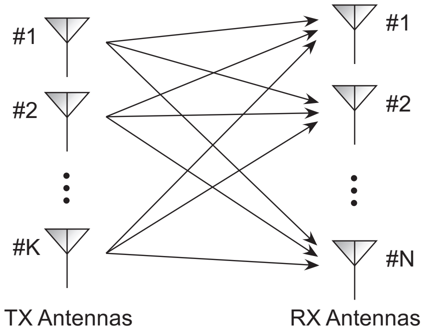

Fig. 1 A model of MIMO-SDM.

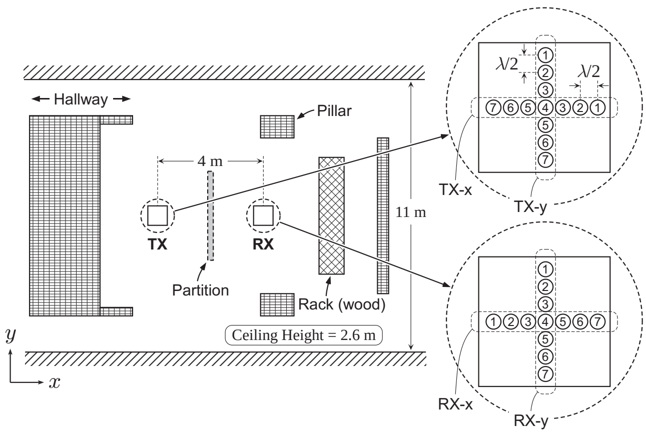

Fig. 2 Measurement environment.

concrete except metal doors. We set TX and RX antennas in this lounge, and measured channel responses by a vector network analyzer. The measurement band was from 5.15GHz to 5.40GHz (250MHz bandwidth). We obtained 1601 frequency-domain data with 156.25kHz interval. We verified statistical stationarity of the propagation in the frequency band. An omnidirectional sleeve antenna was used for each TX and RX antenna, and was mounted on the table as shown in the dotted circles in Fig. 2. Therefore, actual MIMO channel responses were measured without mutual coupling. We set each antenna at the 13 positions on the TX and RX tables with $\lambda/2$ spacing (the half wave length at 5GHz). The TX and RX tables were placed at a distance of 4.0m between the centers of the antenna positions (position ④ in Fig. 2). When we place the metal partition between the TX and RX antennas, we have a NLOS environment. When we remove it, we have a LOS environment. Changing each TX and RX antenna position, a total of $13 \times 13 = 169$ channels were measured in each environment. The measurement campaign was conducted while nobody existed in the lounge.

4. Channel Correlations

To examine the characteristics of measurement environments, we obtained the channel correlations [3] at receiver ends. We define ρ_{ij} which is the correlation between the ith and the jth RX antenna positions by

$$\rho_{ij} = \frac{\sum_{f=1}^{F} \sum_{m=1}^{M} r_{im}(f) r_{jm}^*(f)}{\sqrt{\sum_{f=1}^{F} \sum_{m=1}^{M} |r_{im}(f)|^2} \sqrt{\sum_{f=1}^{F} \sum_{m=1}^{M} |r_{jm}(f)|^2}}, \quad (3)$$

where $r_{im}(f)$ is a channel response from the mth TX antenna to the ith RX antenna at the frequency point f, and the number of total points F is 1601. $r_{jm}(f)$ is defined similarly. Since 13 antenna positions exist at both TX and RX sides, the number of total TX antenna positions M is 13. The range of $|\rho_{ij}|$ is $0 \leq |\rho_{ij}| \leq 1$ because of normalization. We defined the channel correlation matrix $\boldsymbol{R}$ using the $|\rho_{ij}|$. The ith row and the jth column element of $\boldsymbol{R}$ is $|\rho_{ij}|$.

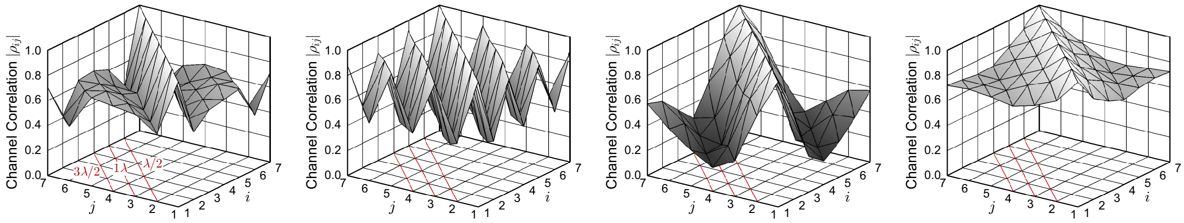

(a) LOS RX-x (b) LOS RX-y (c) NLOS RX-x (d) NLOS RX-y

Fig. 3 Channel correlation matrices $\boldsymbol{R}$ at receiver ends in each environment.

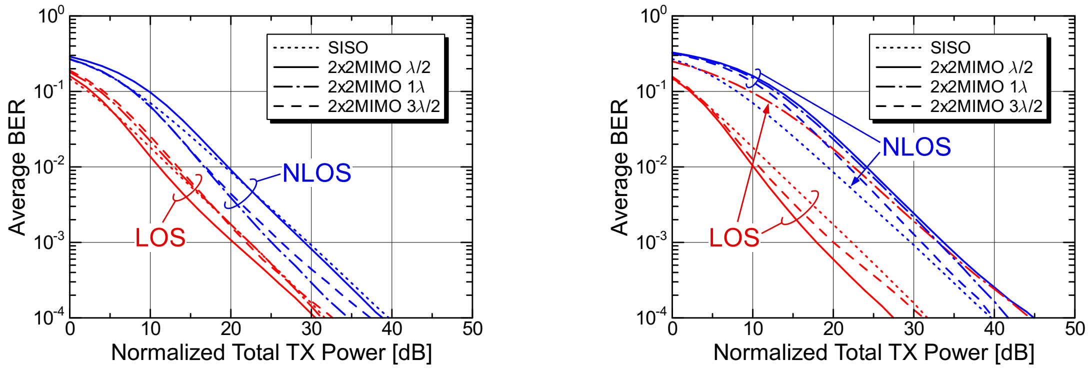

(a) TX-x/RX-x (b) TX-y/RX-y

Fig. 4 Average BER performance of SISO and 2 × 2 MIMO.

Since $|\rho_{ij}| = |\rho_{ji}|$, $\boldsymbol{R}$ is a real-valued symmetric matrix. The channel correlation matrices at receiver ends in LOS and NLOS environments are shown in Fig. 3. Since the x and y directions at the receiver (RX-x, RX-y in Fig. 2) have different propagation characteristics, we evaluated them in each direction. The matrix $\boldsymbol{R}$ is 7×7 because there are 7 antenna positions in each direction. The number of the row or the column corresponds to that of the RX antenna position in Fig. 2, for example, $|\rho_{35}|$ ($|\rho_{53}|$) in RX-x is the value of the channel correlation between the 3rd and the 5th RX antenna positions in RX-x in Fig. 2. Figs. 3 (a) and (b) show the channel correlations of RX-x and RX-y in the LOS channels. Both characteristics have low values at $\lambda/2$ antenna spacing (ex. $|\rho_{12}|$, $|\rho_{23}|$). As for RX-x, the correlations have slightly higher values at 1λ or $3\lambda/2$ than at $\lambda/2$. On the other hand, RX-y correlations have distinct characteristics. They have lower values at $\lambda/2$, $3\lambda/2$, and $5\lambda/2$ spacings, and have higher values at 1λ and 2λ ones. The correlations in the NLOS channels are shown in Figs. 3 (c) and (d). The values in both RX-x and RX-y tend to be lower when the antenna spacing is larger. It is seen that RX-y has generally higher correlations. As for the correlations at transmitter ends, we have almost the same characteristics. The reason for this is conjectured that the lounge (measurement site) has almost symmetric structure.

5. MIMO-SDM Simulation

We generated MIMO channel response matrices $\boldsymbol{H}$ from measured data, and examined the average bit error rate (BER) performance of the V-BLAST processing [1] by simulations. In this case, weights for RX array were determined by the minimum mean square error (MMSE) criterion, and the order of the detection was determined by the mean square error. In the following simulations, we assumed that the MIMO system has 2 TX and 2 RX antennas (2×2 MIMO), and that QPSK modulated signals are transmitted from each TX antenna. There are 4 MIMO system configurations by combinations of TX and RX array directions. In these simulations, the configurations of TX-x/RX-x and TX-y/RX-y were employed. We also evaluated the BER performance of single-input single-output (SISO) systems for comparison with that of MIMO.

Fig. 4 shows the average BER as a function of total transmit power normalized to the value which gives average $E_s/N_0 = 0$ [dB] when a single antenna is used for transmission in an anechoic chamber. As for the MIMO systems, the curves are plotted with a parameter of antenna spacings $\lambda/2$, 1λ, and $3\lambda/2$. The BER curves can be compared with each other in the same total TX power condition. Figs. 4 (a) and (b) show the performance of TX-x/RX-x and TX-y/RX-y, respectively. The curves for SISO are common in both of the figures. As for the TX-x/RX-x case (a), we can see that the LOS channels give better performance than the NLOS ones. In the higher transmit power region (> 20 [dB]), the MIMO performance is better than that of SISO. The $\lambda/2$ antenna spacing MIMO system gives better BER performance than the 1λ and $3\lambda/2$ ones in the LOS cases. The performance of 1λ and $3\lambda/2$ MIMO systems is better than that of $\lambda/2$ one in the NLOS cases. Considering these phenomena together with Figs. 3 (a) and (c), it is seen that MIMO systems with an antenna spacing which has lower channel correlations give better SDM performance. As for the TX-y/RX-y result (b), the BER performance of the

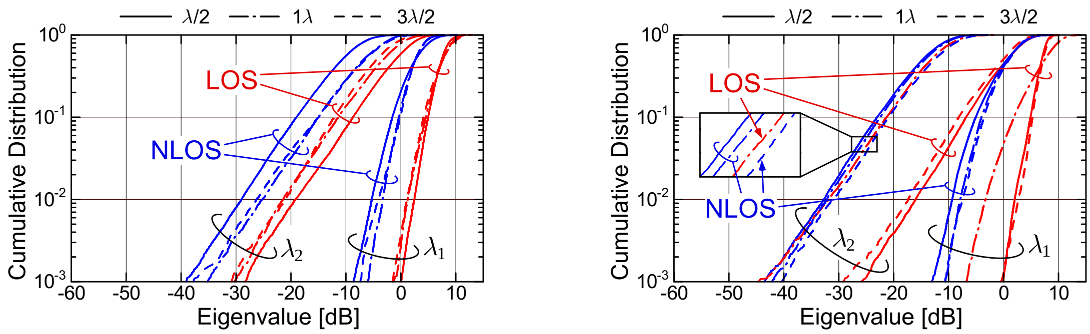

(a) TX-x/RX-x (b) TX-y/RX-y

Fig. 5 Cumulative distributions of eigenvalues for 2×2 MIMO.

MIMO systems with $\lambda/2$ and $3\lambda/2$ spacings is good in the LOS cases. However, the 1λ antenna spacing MIMO system shows significantly poor performance. This deterioration is caused by the correlations as high as about 0.9 at the 1λ spacing as shown in Fig. 3 (b). The correlations are significantly different from those of $\lambda/2$ and $3\lambda/2$ spacings. On the other hand, the performance of TX-y/RX-y in the NLOS cases is poorer than that of TX-x/RX-x in the NLOS ones. This is because the channel correlations of RX-y are generally higher than those of RX-x as shown in Figs. 3 (c) and (d).

6. Eigenvalue Distributions

A $K \times K$ hermitian matrix $\boldsymbol{H}^H\boldsymbol{H}$ has K nonnegative eigenvalues. We represent them in descending order $\lambda_1, \lambda_2, \cdots, \lambda_K$. Note that λ_K is the minimum eigenvalue. The number of positive eigenvalues equals to that of orthogonal channels between the transmitter and the receiver, and the amount of the eigenvalue is in proportion to the signal-to-noise ratio (SNR) of the channel. Therefore, the more large eigenvalues exist, the more data can be transmitted through the channels. Moreover, the smaller the minimum eigenvalue λ_K is, the poorer MIMO-SDM performance tendency is seen. We calculated cumulative distributions of eigenvalues of the 2×2 MIMO systems for the TX-x/RX-x and TX-y/RX-y cases. We have two eigenvalues λ_1 and λ_2. Figs. 5 (a) and (b) show the eigenvalue distributions for the antenna spacings $\lambda/2$, 1λ, and $3\lambda/2$. In general, it is seen that the eigenvalues in the LOS environments are distributed in higher regions than in the NLOS environments. Comparing Fig. 5 with Fig. 4, we see that when the minimum eigenvalue λ_2 has a larger value, better BER performance is obtained.

7. Conclusions

Based on the 5.2GHz measurement campaign in the lounge, the performance of MIMO-SDM in the LOS environments has been compared with that in the NLOS ones. We have examined channel correlations, average BER, and eigenvalue distributions. It has been shown that MIMO-SDM can be utilized in rich multipath LOS environments. However, it has also been shown that the performance of MIMO-SDM in the LOS environments tends to change largely depending on the configuration of antennas (spacing and direction) compared to that in the NLOS environments.

References

[1] G. D. Golden, et al., *Electronics Letters*, vol. 35, no. 1, pp. 14–16, 7th Jan. 1999.

[2] A. F. Molisch, et al., *IEEE J. Select. Areas Commun.*, vol. 20, no. 3, pp. 561–569, Apr. 2002.

[3] H. Özcelik, et al., *IEE 5^{th} EPMCC 2003*, Apr. 2003.

[4] T. Mitsui, et al., *IEEE VTC 2003-Fall*, Oct. 2003.

[5] P. Kyritsi, et al., *IEEE J. Select. Areas Commun.*, vol. 21, no. 5, pp. 713–720, June 2003.

[6] K. Yu, et al., *IEEE GLOBECOM 2001*, vol. 1, pp. 156–160, Nov. 2001.